

Characteristics of Chars from Low-Temperature Pyrolysis of Lignite

Fanrui Meng,[†] Jianglong Yu,^{*,†,‡} Arash Tahmasebi,[†] Yanna Han,[†] Huan Zhao,[‡] John Lucas,[§] and Terry Wall[§]

[†]Key Laboratory of Advanced Coal and Coking Technology of Liaoning Province, School of Chemical Engineering, University of Science and Technology Liaoning, Anshan 114051, People's Republic of China

[‡]Thermal Energy Research Centre, Shenyang Aerospace University, Shenyang 110136, People's Republic of China

[§]Chemical Engineering, University of Newcastle, Callaghan, New South Wales 2308, Australia

ABSTRACT: Low-temperature pyrolysis offers a potential way of upgrading lignite and producing chars to replace thermal or pulverized coal injection (PCI) coals in combustion or being used as inert components in a blend for coking. In this study, the characteristics of chars from low-temperature pyrolysis of two lignite coals have been investigated. The changes in char morphology and chemical structures were investigated using scanning electron microscopy (SEM) and Fourier transform infrared spectroscopy (FTIR). The combustion reactivity of chars was analyzed in a thermogravimetric analyzer (TGA) using non-isothermal techniques. The results show that chars from low-temperature pyrolysis of lignite coal below 450 °C were more reactive than higher temperature chars. Higher reactivity of low-temperature chars was attributed to the higher concentration of active sites and lower degree of structural order compared to that of high-temperature chars. Indonesian (YN) lignite showed a higher weight loss rate compared to Hulunbeier (HL) coal, which was attributed to a higher concentration of liptinite and vitrinite in YN coal. FTIR analysis indicated that the aliphatic structures and oxygen-containing functional groups decreased with an increasing pyrolysis temperature. The intensity of tightly bound cyclic OH tetramers and OH–ether O hydrogen bonds were higher than other hydrogen bonds in the 3700–3600 cm⁻¹ region of infrared (IR) spectra. The density of alkyl chains and cross-linking reactions affected the yield of tar. The aromaticity of char increased with an increasing pyrolysis temperature. The abundance of C=O and COOH structures decreased drastically with increasing temperature. A lower concentration of active sites on high-temperature chars resulted in lower combustion reactivity compared to low-temperature chars. The C–O and C=C groups decreased as the temperature increased possibly because of the aromatic condensation. The extent of aromatic substitution decreased up to 650 °C. At temperatures above 650 °C, the degree of aromaticity was strengthened and larger condensed aromatic nuclei were formed. Brunauer–Emmett–Teller (BET) surface area analysis revealed that high-temperature chars have significantly higher surface area compared to chars produced at low temperatures. However, the concentration of active sites was lower in high-temperature chars. Therefore, it can be concluded that diffusion was the main reaction mechanism in high-temperature chars.

1. INTRODUCTION

Low-temperature pyrolysis of coal is regarded as an effective way to upgrade low-rank coals, such as lignite. It is also a common way to produce volatile matter products, typically light gases and tars, and an appropriate way for low-temperature carbonization.^{1,2} Chars from low-temperature pyrolysis of lignite may be used to replace thermal coals or pulverized coal injection (PCI) coals in combustion or as inert components in a blend for coking. The combustion characteristics of char can directly affect burnout and, therefore, the unburned carbon content in ash.³ The combustion of char involves several steps, including the diffusion of oxygen to active sites on the char surface, chemisorption of oxygen on the char surface, internal diffusion of oxygen from the surface to the porous matrix, reaction of chemisorbed oxygen with carbon to form products, and desorption of products from the char surface. The combustion rate of char would thus be dependent upon the slowest step.^{3–5} The release of volatiles alters the macromolecular network of coal, which affects the reactivity of char. Therefore, the extent of coal devolatilization during pyrolysis has a significant effect on morphology and molecular structure formation of char.^{6,7}

A number of techniques to characterize chars are cited in the literature, including ¹H nuclear magnetic resonance (NMR), Fourier transform (FT)-Raman, Fourier transform infrared spectroscopy (FTIR), thermogravimetric analysis (TGA), etc.^{8–12} Among them, the FTIR technique has been used to examine organic functional groups, such as carbonyl, aromatic/aliphatic hydrogen, and carbon groups,^{6,12–19} while TGA was widely employed to analyze the reactivity of chars.^{3,4,20} Mastral et al.¹⁸ analyzed the first stages of char formation during pyrolysis using different analytical techniques. The chars of low-temperature pyrolysis were obtained at 400 °C at different residence times, and their results showed the disappearance of the aliphatic hydrogen content with increasing pyrolysis time. Ibarra et al.^{6,19} investigated the influence of functional groups in coal on cross-linking reactions during pyrolysis. They claimed that the cross-linking reactions affect the evolution of tar and

Special Issue: 4th (2013) Sino-Australian Symposium on Advanced Coal and Biomass Utilisation Technologies

Received: July 24, 2013

Revised: October 21, 2013



gaseous species, such as CO_2 , CH_4 , and H_2O . The degree of aromatic substitution decreased and aromatic hydrogen tended to increase with an increasing pyrolysis temperature. Khan et al.⁴ investigated the reactivity of coal chars prepared at 500 and 750 °C. They postulated that the hydrogen content of chars greatly affects their reactivity. Wells et al.²¹ reported the order of importance of the variables on char reactivity, i.e., catalysis > porosity > total hydrogen. Physical and structural characteristics of the char strongly influence carbon burn-out.⁹ Sadhukhan et al.²² reported that the combustion characteristics of coal char are highly dependent upon the initial pore structure of devolatilized char as well as the structural evolution during the combustion of char. Haykiri-Acma et al.³ reported that increasing the final temperature in pyrolysis reduced the combustion reactivity of the char. Chars from low-temperature pyrolysis of lignite, which is currently used as a means of upgrading lignite in China, have not been systematically studied in the literature. In this study, we investigated the characteristics of chars obtained from low-temperature pyrolysis of two lignite coals using FTIR, thermogravimetry (TG), and scanning electron microscopy (SEM). The effects of changes in functional groups on char combustion reactivity are studied in detail.

2. EXPERIMENTAL SECTION

2.1. Coal Sample Preparation. Two lignite coals, Hulunbeier (assigned as HL, from Inner Mongolia, north China), and Indonesian

Table 1. Proximate and Ultimate Analyses and Petrographic Composition of the Coal Samples

coal sample ^a	HL	YN
moisture content (wt %, ad)	14.88	20.38
volatile matter (wt %, ad)	33.98	38.87
ash (wt %, ad)	10.3	6.02
fixed carbon (wt %, ad)	39.02	34.73
C (wt %, db)	61.99	69.3
H (wt %, db)	5.05	4.79
N (wt %, db)	0.8	1.0
S (wt %, db)	0.26	0.24
O (by difference) (wt %, db)	17.66	21.6
vitrinite (%)	63.4	78.2
inertinite (%)	24.6	10.8
liptinite (%)	1.7	4.2

^aad, air dried; db, dry basis.

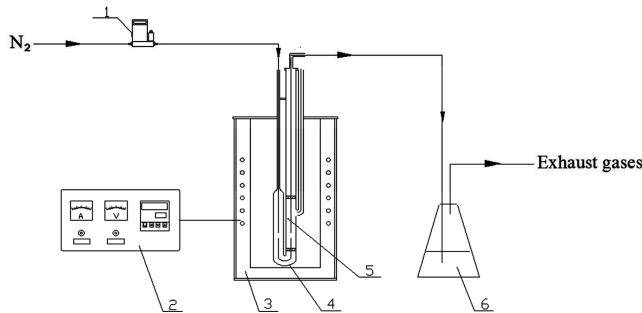


Figure 1. Schematic diagram of the pyrolysis experimental setup: (1) mass flow controller, (2) temperature controller, (3) furnace, (4) quartz reactor, (5) coal sample, and (6) condenser.

lignite (assigned as YN, supplied by Banpu Public Company, Ltd., Thailand), were used in this study. The proximate and ultimate

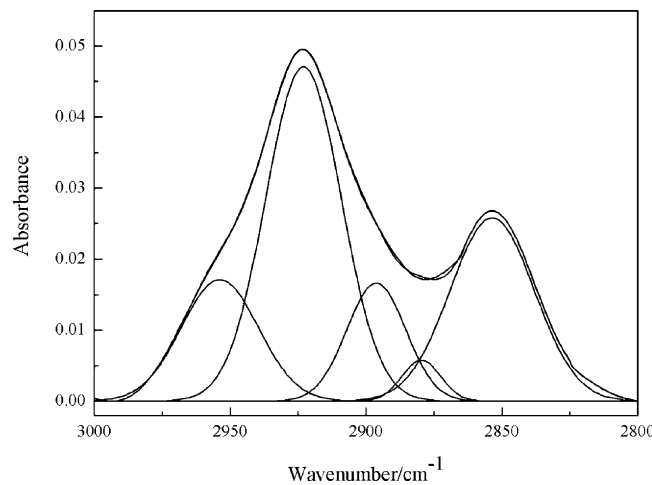


Figure 2. Curve-fitted spectra of the 3000–2800 cm^{-1} zone for HL coal.

analysis data and petrographic composition are given in Table 1. Both coals have high volatile matter and moisture contents. YN coal has lower ash content compared to HL coal. Petrographic analysis showed that YN lignite contained more vitrinite and liptinite compared to HL lignite. The coal samples were stored under an oxygen-free atmosphere in airtight plastic bags in a fridge. About half of the raw coals were crushed and sieved to less than 0.2 mm by a jaw crusher and vibrating screen, respectively, and stored in sealed and oxygen-free sample containers in the fridge.

2.2. Pyrolysis Experiments. The pyrolysis experiments were carried out in a vertical fixed-bed tubular quartz reactor with an internal diameter of 2.0 cm heated by an electric furnace. Nitrogen was used as the carrier gas with a gas flow rate of 200 mL/min. A total of 5.0 g of the samples was used for every pyrolysis experiment. When the furnace was heated to pyrolysis temperatures (350, 400, 450, 500, 550, 600, 650, 700, and 750 °C), the reactor loaded with coal samples was put into the furnace and heated for 30 min. All of the experimental runs were repeated at least 3 times to ensure the reproducibility of the results. The experimental error ranged between $\pm 5\%$ of the mean value. The experimental setup is shown in Figure 1.

The pyrolysis product yields were calculated using the following equations:^{23,24}

$$Y_{\text{char}} = \frac{W_{\text{char}} - W_0 A}{W_0(1 - A - M)} \times 100\% \quad (1)$$

$$Y_{\text{tar}} = \frac{W_{\text{tar}}}{W_0(1 - A - M)} \times 100\% \quad (2)$$

$$Y_{(\text{gases})} = (1 - Y_{\text{tar}} - Y_{\text{char}}) \times 100\% \quad (3)$$

where W_{char} is the weight of char obtained during experiments, W_0 is the initial weight of the coal sample, W_{tar} is the weight of tar obtained from experiments, A is the ash content, and M is the moisture content of coal (wt %, ad basis).

2.3. Char Combustion Reactivity. The combustion experiments were carried out using a thermogravimetric analyzer (PerkinElmer Diamond TG/DTA 6300). In combustion experiments, 5 ± 0.1 mg of sample was heated from room temperature to a maximum temperature of 800 °C at the heating rate of 10 °C/min under air conditions.

The reactivity index (R) of the char was calculated from eq 4.^{25,26} This definition is widely used in the literature for comparison of reactivity of different coals

$$R = \frac{0.5}{t_{0.5}} \quad (4)$$

where $t_{0.5}$ is the time required to reach fixed-carbon conversion of 50 wt %. This index represents reactivity over a relatively wide range of

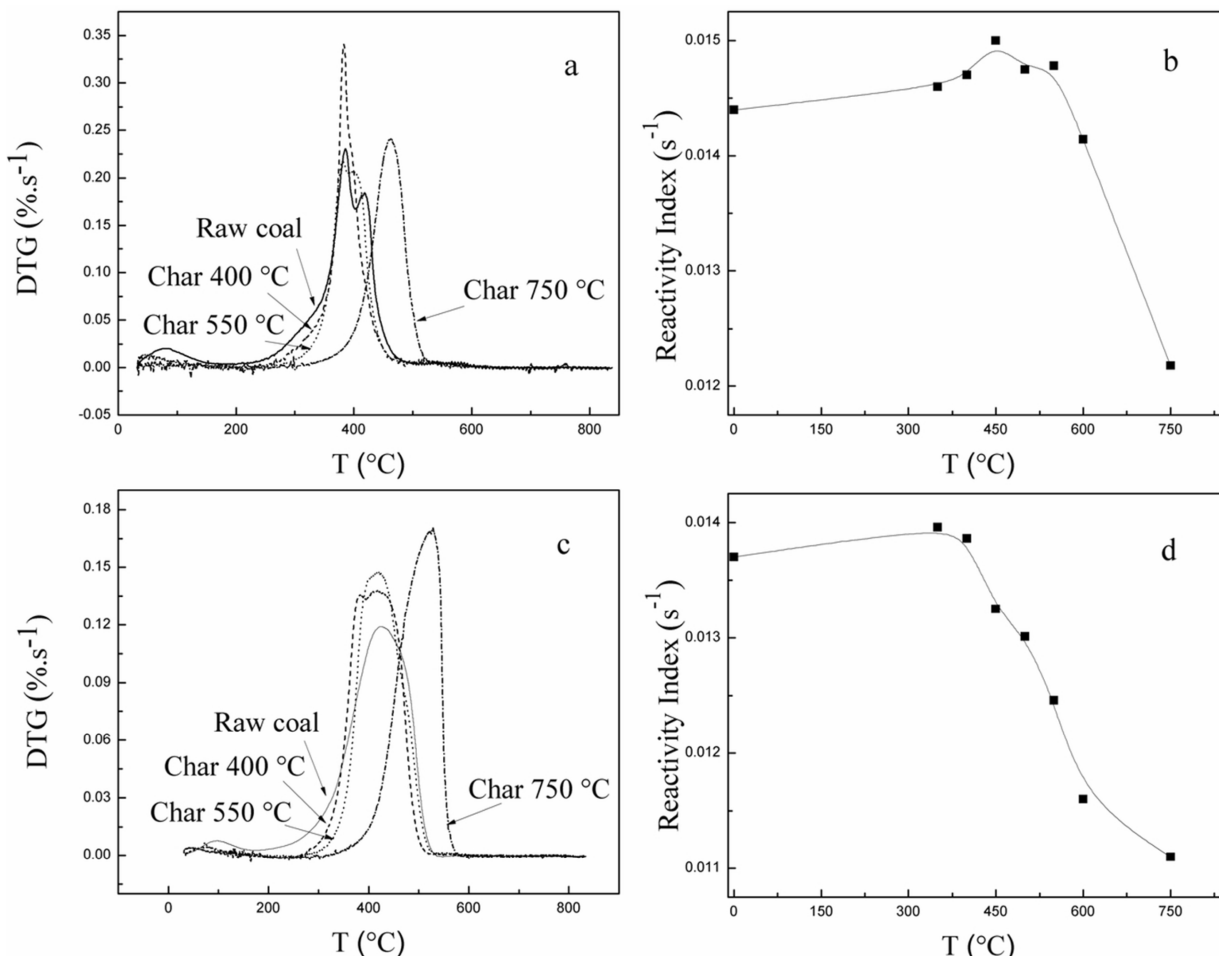


Figure 3. DTG curves and combustion reactivity (R) of raw coals and chars: (a and b) HL coal and (c and d) YN coal.

conversion. R is the average reaction rate from 0 to 50 wt % conversion.²⁵

2.4. Char Characterization. The surface morphology of coal and char samples was analyzed using SEM (JEOL JSM-6480LV). The BET surface area of different coal and char samples was measured with a specific surface area and pore size analyzer (V-sorb 4800 P). The N_2 gas adsorption method at 77 K was used. The coal and char samples were first oven-dried at 105 °C and then degassed in the adsorption system at 200 °C to a final pressure of 1.33×10^{-4} Pa. To ensure the reproducibility and accuracy of analysis, experiments were repeated 3 times and the average values are reported. The Barrett–Joyner–Halenda (BJH) model was used to determine the pore size distributions from the desorption isotherm.

Infrared (IR) spectra of the coal and char samples were obtained using a FTIR spectrometer (Thermo Scientific Nicolet iSS). Prior to FTIR analysis, KBr and samples were dried in the vacuum oven for 12 h to prevent the effect of water on the results. KBr pellets were prepared by grinding the mixture of 1 mg of sample with 120 mg of KBr. IR spectra of the coal samples for the 4000–400 cm^{-1} region were studied by curve-fitting analysis using a commercially available data-processing program (OriginPro, OriginLab Corporation). Prior to FTIR measurements, a reference spectrum was obtained from pure KBr pellets without the addition of any coal. Assignment of the bands in the IR spectra was made according to the literature and is presented in Table 3.^{6,12,16,17,27–30} Prior to curve-fitting analysis, the mineral matter corrections were applied on IR spectra, as suggested in the literature.^{31–33} HL and YN ash samples were obtained by combustion at 500 °C. Combustion was performed at low temperatures to prevent the change in ash composition. The IR spectra of ash samples were subtracted from the corresponding coal and char samples, and the ash-

free IR spectra of samples were further analyzed by curve-fitting analysis. The extinction coefficients used for converting integrated absorbance areas to concentration units were 541 and 710 $\text{abs cm}^{-1} \text{mg cm}^{-2}$ for the aromatic and aliphatic bands for HL and YN coal, respectively, and 684 and 744 $\text{abs cm}^{-1} \text{mg cm}^{-2}$ for char.^{12,34,35} Initial approximation of the number of bands and peak positions was obtained by examining second derivatives of the spectral data, and Gaussian functions were used as mathematical functions.¹² An example of the curve-fitted spectra for HL coal in 3000–2800 cm^{-1} is shown in Figure 2, and the results are presented in Table 4. The coefficient of determination (COD) was the primary criterion in examining the goodness of curve fitting. COD values of the curve-fitting analysis in all cases were all above 0.999, indicating that IR spectra of all samples were curve-fitted with high accuracy.

3. RESULTS AND DISCUSSION

3.1. Combustion Reactivity of Low-Temperature Pyrolysis Chars. Non-isothermal combustion reactivity of HL and YN coals and chars prepared at 400, 550, and 750 °C is compared in Figure 3. The differential thermogravimetry (DTG) curves showed that the temperature corresponding to the initial weight loss (200–350 °C) increased with an increasing pyrolysis temperature, indicating that the thermal output of devolatilization has an influence on char combustion reactivity. With increasing temperature, the volatile matter content decreased, resulting in the increased ignition temperature. The maximum reaction rates of chars were greater than those of the raw coals. It is been suggested that, because of the higher porosity of chars compared to that of raw coals, the

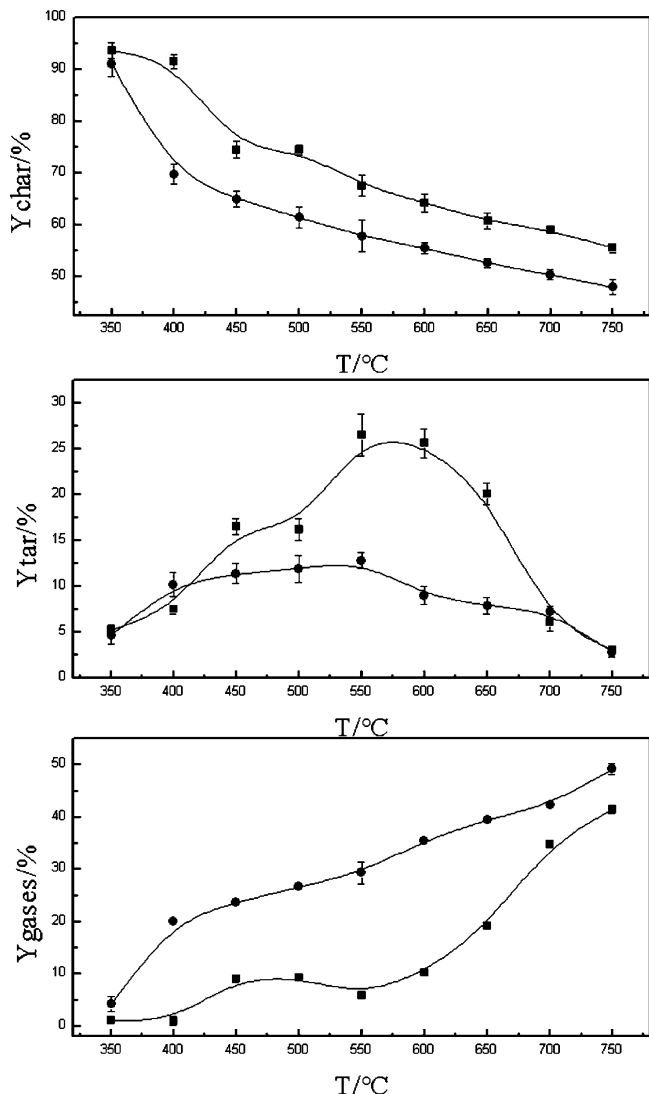


Figure 4. Yields of pyrolysis products after 30 min of pyrolysis at different temperatures: (■) HL coal and (●) YN coal.

oxygen diffusivity into the char structure increases, resulting in higher combustion reactivity.^{4,36} Figure 3 also shows the combustion reactivity of HL and YN coals and their chars as a function of the char preparation temperature calculated using eq 4. It can be seen that the combustion reactivity (*R*) of low-temperature chars (350–450 °C for HL coal and 350–400 °C for YN coal) was greater than that of corresponding raw coals and the higher temperature chars. The difference in reactivity of chars prepared at different temperatures can be attributed to the difference in physical and chemical structures of these chars. Effects of physical and chemical structures of chars on their combustion reactivity are discussed in detail in the following sections.

3.2. Yields of Pyrolysis Products. When coal is heated, some bridging bonds in its macromolecular network break down, generating tar and noncondensable gases.¹⁸ Figure 4 shows the effects of the pyrolysis temperature on product yields. The char yield decreased rapidly with an increasing temperature to 74% at 450 °C for HL coal and 65% at 400 °C for YN coal, followed by a gradual decrease to 56 and 47% at 750 °C for the HL and YN coals, respectively. The tar yield increased to its maximum at 550 °C for both coals and

decreased thereafter. The gas yield increased monotonically with an increasing pyrolysis temperature. The char and tar yields for HL coal were higher compared to YN coal. It has been reported in the literature that the volatile yield from individual macerals in coal is different, with liptinite giving the highest yield, followed by vitrinite and inertinite.^{37–39} As seen in Table 1, the concentration of both liptinite and vitrinite was higher in YN coal (4.2 and 78.2, respectively) compared to that in HL coal (1.7 and 63.4, respectively), which resulted in a higher rate of pyrolysis and volatile yield.

3.3. Morphology and Surface Area Analysis of Chars from Low-Temperature Pyrolysis. The SEM images of HL and YL coals and char samples prepared at different pyrolysis temperatures are shown in Figure 5. SEM analysis of the raw coals showed that the particles had a rough surface (panels a and g of Figure 5). At 350 °C, many pores were observed on the char surface because of the volatile release (panels b and h of Figure 5). At 450 °C, the char particles developed cracks as a result of the volatile matter release (panels c and i of Figure 5). From Figure 4, it can be seen that the tar, water, and gas yields increased rapidly at 450 °C, suggesting that the rate of volatile release was accelerated by increasing temperature. The release of volatile matter within the softened coal matrix resulted in the formation of macropores and vesicles (panels b and h of Figure 5). New channels were formed inside particles because of the expansion of the inner hole. Fractures were formed on the particle surface because of thermal expansion, resulting in pore collapse and blockage, as seen in panels c and i of Figure 5.⁴⁰ Panels d–f and j–l of Figure 5 showed a gradually smoothed particle surface with increasing pyrolysis temperatures above 550 °C. For chars prepared at above 600 °C, the organic matter of char underwent further decomposition. Particles had amorphous shapes at 750 °C. According to the literature, at high temperatures, the carbon net structure increases and possesses a higher degree of structural order.^{8,9,36,41,42} At 750 °C, some cracks were observed on the char particle surface (panels f and l of Figure 5), suggesting that the char structure underwent contraction and densification.^{5,43} The increase of the pyrolysis temperature enhanced coal plasticity, and a more extensive consolidation during the metaplast stage of pyrolysis occurred, leading to lower char reactivities at a higher pyrolysis temperature.^{44,45}

The porosity in the char structure depends upon a balance between additional pore volume created by volatile matter release and loss of the pore volume caused by enhanced alignment and growth of the planar building blocks.⁴⁶ The changes in the pore structure and specific surface areas of coal will affect the reactivity of char during gasification or combustion. As shown in Table 2, the surface areas and pore volume of HL coal increased with an increasing pyrolysis temperature, indicating that the release of volatile matter during the pyrolysis process resulted in the formation of internal porosity. However, reactivity analysis in Figure 3 showed that chars prepared at 400–450 °C had the highest combustion reactivity. Therefore, the evolution of chemical structures was investigated to study the effect of the functional group concentration on char reactivity.

3.4. Chemical Structure Changes during Pyrolysis. The IR spectra of samples are shown in Figure 6. Remarkable changes occurred in the regions of 3700–3000 cm⁻¹ (OH), 3000–2800 cm⁻¹ (aliphatic C–H), 1800–1000 cm⁻¹ (C=O, COOH, C=C, and C–O), and 900–700 cm⁻¹ (aromatic C–H out of plane). The disappearance of observable structural

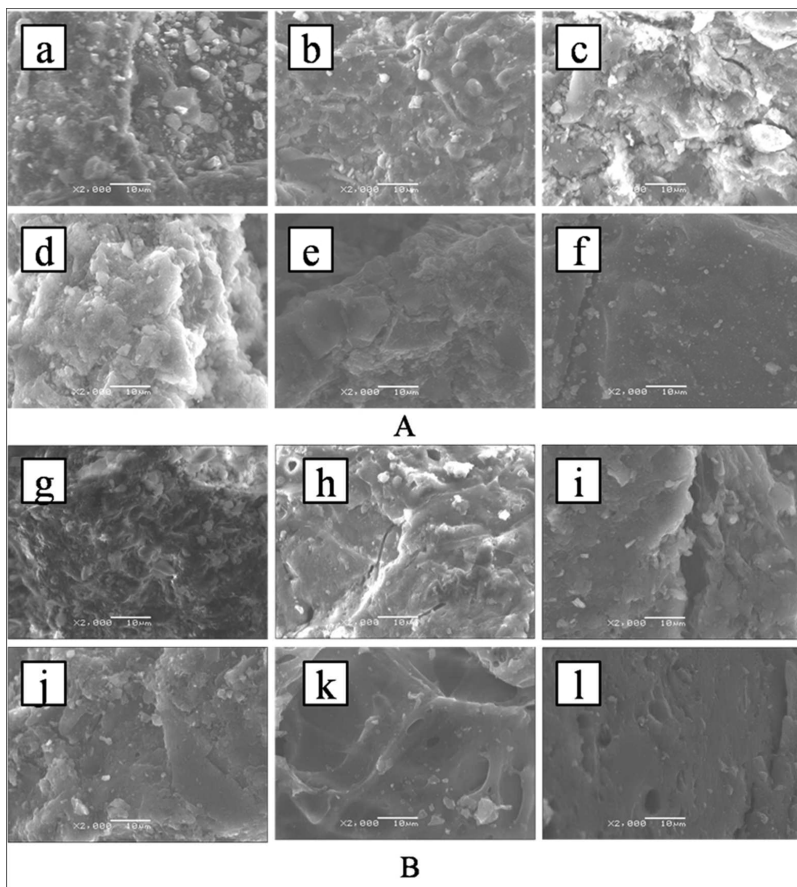
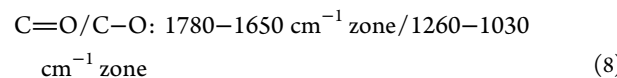
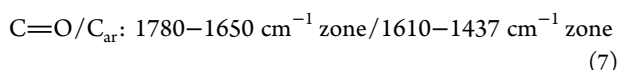
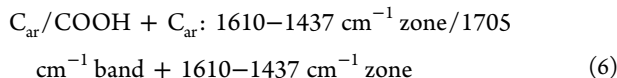
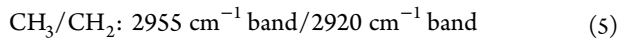


Figure 5. SEM images of morphology of coals and chars from pyrolysis at different temperatures: (A) HL coal and its chars, (B) YN coal and its chars, (a and g) raw coal, (b and h) char at 350 °C, (c and i) char at 450 °C, (d and j) char at 550 °C, (e and k) char at 650 °C, and (f and l) char at 750 °C.

Table 2. Surface Areas and Pore Volume of HL Coal and Its Char Samples

	raw coal	char at 400 °C	char at 550 °C	char at 750 °C
surface area (m ² /g)	4.52	5.07	6.27	92.56
pore volume (cm ³ /g)	0.020	0.024	0.026	0.023

features was related to intense release of volatiles during pyrolysis and the loss of functional groups.⁴⁵ To further investigate the structural modifications of lignite coals during pyrolysis, the selected zones of the IR spectra of coals and chars were studied by curve-fitting analysis. The band positions and assignments in the FTIR spectra of the samples are listed in Table 3. From the curve-fitted bands, a series of parameters was defined as ratios of integrated absorbance areas and was used to quantify the structure changes of coal during pyrolysis. The relationships investigated are given in the following:



Equation 5 shows the ratio of methyl/methylene structures, and it can be considered as an estimate of the length of aliphatic chains of coal.^{6,12,27} Equation 6 depicts the ratio of aromatic/carboxylic groups as a suitable index for assessing the degree of maturation of organic matter.^{12,47} Equations 7 and 8 provide a quantitative estimate of the changes of carboxylic, carbonyl, and other C–O structures in relation to the aromatic macromolecular network of coal.¹² The calculated parameters as a function of the pyrolysis temperature are listed in Table 5.

3.4.1. OH-Associated Hydrogen Bonds. The 3700–3000 cm⁻¹ zone of the IR spectra of samples revealed the presence of six bands in this region (Table 3); five of these bands were attributed to OH structures. Similar results have been reported in the literature.^{28–30} Figure 7 shows the changes of hydrogen bond adsorption as a function of the pyrolysis temperature. The concentration of free OH groups, OH–π hydrogen bonds, and self-associated OH groups reached nearly zero after pyrolysis at temperatures higher than 450 °C. This suggests that these hydrogen bonds are weaker than tightly bound cyclic OH tetramers and OH–ether O hydrogen bonds. The concentration of self-associated OH groups of YN char was higher than that of HL char at the temperature range of 350–450 °C. This was probably due to two reasons. One reason is probably due to the sensitivity of FTIR to water. The intense bands at 3416–3400 cm⁻¹ are attributed to OH from H₂O or phenol

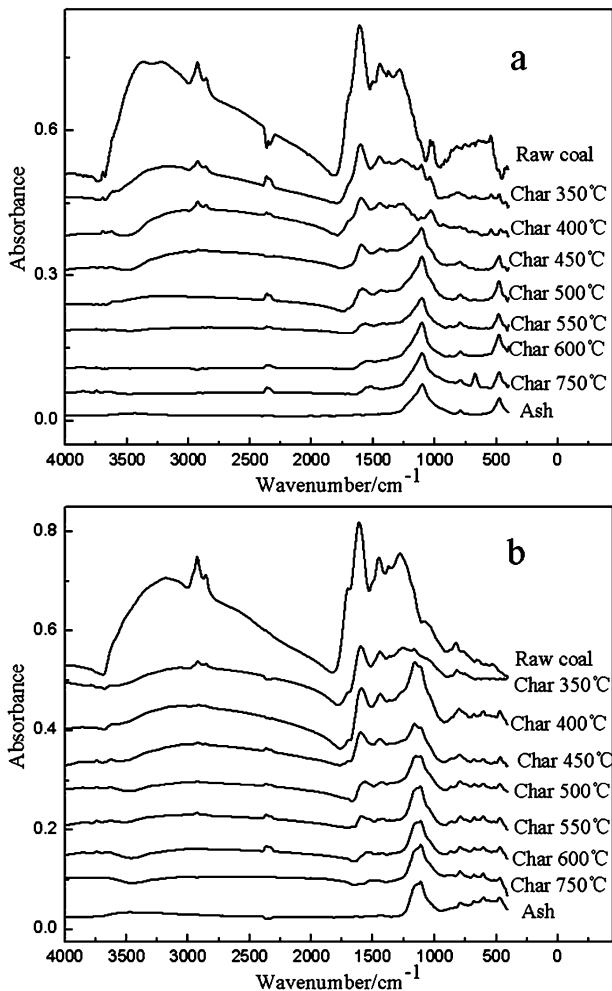


Figure 6. FTIR spectra of lignite coals and chars: (a) HL coal and its chars and (b) YN coal and its chars.

groups.^{48,49} The other reason is probably due to the breakage of the tightly bound cyclic OH tetramers. Figure 7b shows that the content of cyclic OH tetramers is higher than self-associated OH groups in YN coal, suggesting that the cyclic OH tetramers were broken into self-associated OH groups during the pyrolysis process. Because of the weaker hydrogen bond, the self-associated OH groups decrease dramatically above 400 °C. The water that is evolved during pyrolysis probably arises mainly from the condensation of OH groups, and the activation is strong when the hydrogen bonds break or cross-link.⁵

3.4.2. Changes in Aliphatic Structures. As seen in Figure 6, the intensity of bands in the aliphatic C–H (3000–2700 cm⁻¹) zone progressively decreased with an increasing pyrolysis temperature for both HL and YN coals. Aliphatic structures were practically all removed above 550 °C. Figure 8 shows the curve-fitted IR spectra of the 3000–2700 cm⁻¹ zone for HL coal and its char prepared at 500 °C. The position and assignment of bands for raw coal are listed in Table 3.^{6,12,14} The aliphatic region of the raw coal can be curve-fitted to a series of five bands attributed to asymmetric –CH₃ and –CH₂– stretching (2953 and 2923 cm⁻¹, respectively), symmetric –CH₃ and –CH₂– stretching (2879 and 2853 cm⁻¹, respectively), and methine C–H stretching (2896 cm⁻¹), as shown in Figure 8a. The results are presented in Table 4. With increasing temperature, changes in intensity, position, and

Table 3. Band Positions and Assignments in the FTIR Spectra of Lignite Samples^a

position (cm ⁻¹)	assignments	position (cm ⁻¹)	assignments
	a		c
3610	free OH groups	895	1H
3516	OH–π hydrogen bonds	876	1H
3400	self-associated <i>n</i> -mers (<i>n</i> > 3)	860	1H
3300	OH–ether O hydrogen bonds	838	2H
3200	tightly bound cyclic OH tetramers	815	2H
3050	aromatic hydrogen	790	3H
	b	750	4H
2953	asymmetric RCH ₃	742	4H
2923	asymmetric R ₂ CH ₂	720	(CH ₃) _{<i>n</i>≥4}
2896	R ₃ CH	695	5H
2879	symmetric RCH ₃		
2853	symmetric R ₂ CH ₂		
	d		
1772	aryl esters	1410	asymmetric CH–(CH ₃); OH
1703	carboxyl acids	1377	symmetric CH ₃ –Ar, R
1650	conjugated C=O	1350	symmetric CH ₂ –C=O
1610	aromatic C=C	1274	C–O in aryl ethers
1586	aromatic C=C	1222	C–O and OH, phenoxy structures, ethers
1500	aromatic C=C	1168	C–O phenols, ethers
1458	asymmetric CH ₃ –, CH ₂ –	1094	C–O secondary alcohols
1437	aromatic C=C	1036	alkyl ethers

^a(a) Hydrogen bonds formed by OH groups in coal, (b) aliphatic C–H stretching; (c) aromatic C–H out-of-plane deformation bands, and (d) curve-fitted bands for the 1800–1000 cm⁻¹ region.

appearance of new bands can be observed. Figure 8b shows the curve-fitting for the aliphatic bands of char prepared at 500 °C from HL coal. New bands can be observed at 2836, 2881, and 2904 cm⁻¹. The 2904 cm⁻¹ band can be assigned to methyl groups. According to Wang and Griffiths,¹³ this band could be assigned to CH₃–CO groups. The 2881 cm⁻¹ band can be attributed to methine groups.⁶ The 2836 cm⁻¹ band has also been reported in the literature,^{13,14} but it has not been identified. Similar results were obtained for YN coal and its chars.

The variation of the methyl (2953 cm⁻¹) and methylene (2923 cm⁻¹) bands was examined, and the results are given in Table 5. HL coal has a lower methyl/methylene ratio than YN coal, indicating the presence of a larger number of alkyl chains in HL coal. The presence of a larger number of alkyl chains in HL coal resulted in higher yields of tar from HL coal (Figure 4).⁵⁰ Below 450 °C, the methyl/methylene ratio of HL coal increases because of the decrease of the alkyl chains. At 450 °C, a significant change in the ratio for HL coal occurred because of the tar release (Table 5 and Figure 4). Methyl structures (2953 cm⁻¹) were all removed above 450 °C. For YN coal, the change in the methyl/methylene ratio occurred at 350 °C. While the methyl/methylene ratio decreased gradually with increasing temperature, the tar production from YN coal was lower than HL coal but the gas and water yields were higher for YN coal (Figure 4). The release of gaseous species, such as H₂O, CO₂, CO, and CH₄, occurred simultaneously with the cross-linking

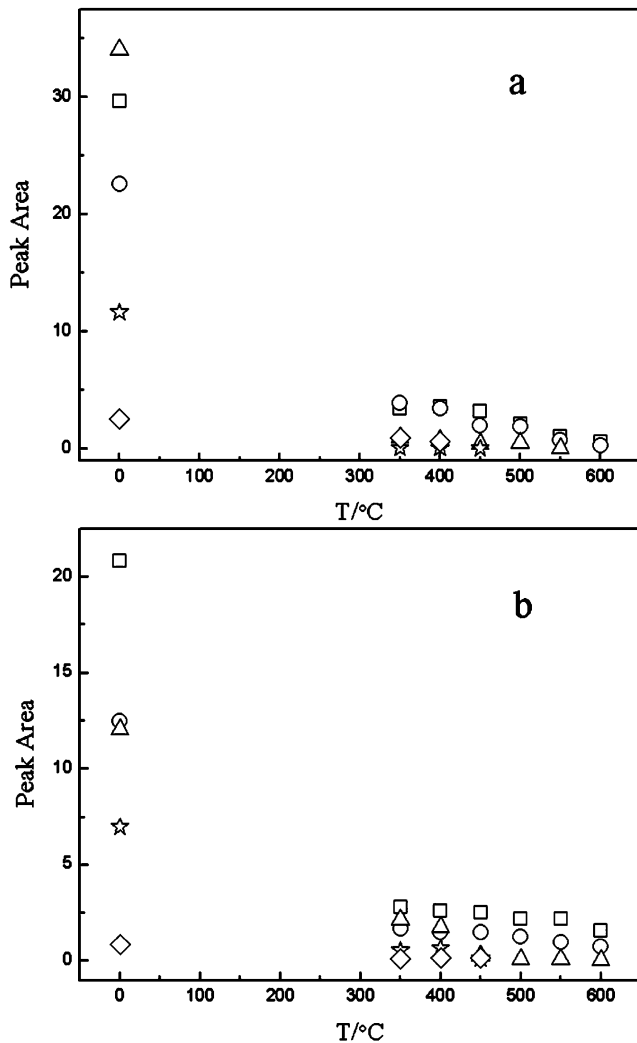


Figure 7. Changes in hydrogen bonds formed by OH group adsorption as a function of the pyrolysis temperature: (a) HL coal and (b) YN coal, (□) tightly bound cyclic OH tetramers, (○) OH–ether O hydrogen bonds, (△) self-associated OH, (☆) OH– π hydrogen bonds, and (◊) free OH groups.

reactions in coal pyrolysis.^{6,19,20,51,52} Cross-linking in lignite occurs at lower temperatures compared to higher rank coals, and more cross-links lead to lower yields of tar.¹⁵ Solomon et al.¹⁵ reported that the cross-linking reactions occur with the loss of carboxyl groups present in the coal.

3.4.3. Alteration of Oxygen-Containing Structures. The 1800–1000 cm⁻¹ zone showed the most significant differences in HL and YN coals. The second-derivative analysis of this zone revealed the presence of 16 bands (Table 3).^{12,48} Figure 9 shows the changes of aromatic C=C, carbonyl, carboxyl, and C–O group adsorption as a function of the pyrolysis temperature. The adsorption of C=O and COOH structures decreased drastically with increasing temperature (Table 5). The loss of active sites on the char surface decreased the combustion reactivity of high-temperature chars (Figure 3). The presence of oxygen functional groups is the main reason for low-temperature cross-linking reactions in low-rank coals.¹⁵ It can be seen in Figure 9 that, with increasing temperature to 400 °C, the carboxyl groups decreased by 90.6 and 82.9% for YN and HL coals, respectively, indicating that the cross-linking for YN coal occurs at a lower temperature compared to HL

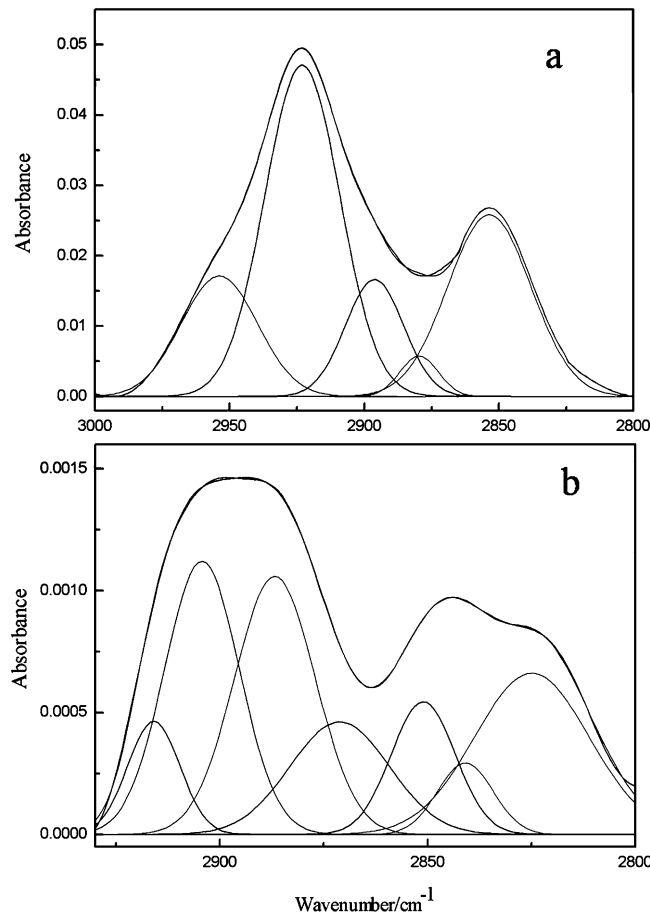


Figure 8. Curve-fitted IR spectrum of the aliphatic C–H stretching bands for HL raw coal and (b) char at 500 °C.

Table 4. Curve-Fitting for the Aliphatic C–H Stretching Bands of HL Raw Coal

center (cm ⁻¹)	assignment	width (cm ⁻¹)	height ^a	area ^b
2853	asymmetric RCH ₃	36.45	0.026	1.002 ± 0.003
2879	asymmetric R ₂ CH ₂	16.92	0.006	0.103 ± 0.001
2896	R ₃ CH	25.57	0.017	0.453 ± 0.004
2923	symmetric RCH ₃	32.78	0.047	1.679 ± 0.042
2953	symmetric R ₂ CH ₂	33.42	0.017	0.608 ± 0.001

^aAbsorbance units. ^bIntegrated absorbance unit × cm⁻¹.

coal. A lower tar yield during pyrolysis of YN coal compared to that of HL coal (Figure 4) can therefore be attributed to higher cross-linking reactions at temperatures lower than the tar-release temperature.¹⁹

The C–O groups decreased considerably below 350 °C for studied coals, which may be attributed to the presence of lignin-like structures inferred from the bands at 1274 cm⁻¹ (aryl ethers).¹² At the temperature range of 450–650 °C, the C–O groups were relatively stable but decreased at temperatures above 650 °C, indicating that ether is the important link for aromatic condensation. It can be seen in Figure 6 that the band over 1610 cm⁻¹ (C=C stretching vibrations) decreased with an increasing pyrolysis temperature.^{12,16,48} The 1610 cm⁻¹ band may not be detected by FTIR at high temperatures.⁵³ Carbonyl groups partially overlap with the adsorption of the aromatic ring.^{48,54} The vibrations of groups giving rise to the 1610 cm⁻¹

Table 5. Structural Parameters Derived from the Curve-Fitting Analysis of the FTIR Spectra

parameter	sample	pyrolysis temperature (°C)							
		raw coal	350	400	450	500	550	600	650
CH_3/CH_2	HL	0.37	0.45	0.43	0.16				
	YN	1.32	0.23	0.39	0.24	0.20	0.18		
$\text{C}_{\text{ar}}/\text{COOH} + \text{C}_{\text{ar}}$	HL	0.87	0.91	0.92	0.99				
	YN	0.77	0.94	0.96					
C=O/C_{ar}	HL	0.26	0.17	0.16	0.11	0.11	0.01		
	YN	0.39	0.11	0.06	0.06				
C=O/C-O	HL	0.37	0.16	0.13	0.06	0.07	0.05	0.01	
	YN	0.36	0.08	0.05	0.04				

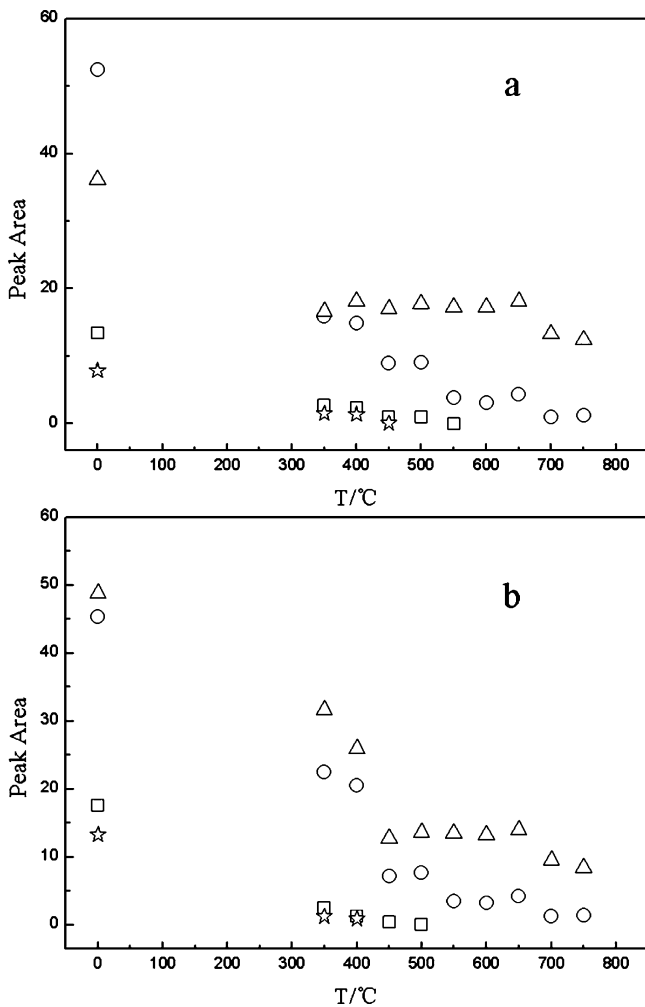


Figure 9. Changes in aromatic $\text{C}=\text{C}$, carbonyl, carboxyl, and $\text{C}-\text{O}$ group adsorption as a function of the pyrolysis temperature: (a) HL coal and (b) YN coal, (\square) carbonyl, (\circ) aromatic $\text{C}=\text{C}$, (\triangle) $\text{C}-\text{O}$, and (\star) carboxyl groups.

band are IR-active when their symmetry is distorted by adjacent functional groups containing oxygen.⁵⁵ Because C=O and $\text{C}-\text{O}$ species are progressively destroyed during pyrolysis with increasing temperature, adjacent $\text{C}=\text{C}$ groups at 1610 cm^{-1} become symmetrical and IR-inactive and disappear. In this study, the integrated absorbance area of $\text{C}=\text{C}$ groups ($1610\text{--}1437\text{ cm}^{-1}$) was used to describe the evolution of the $\text{C}=\text{C}$ structure. With increasing temperature, more stable structures, such as alkyl–aryl $\text{C}-\text{C}$, may form from the $\text{C}=\text{C}$ structures as a result of cross-linking reactions following the decarboxylation

reactions or the loss of other O-containing functional groups.⁵⁶ The $\text{C}_{\text{ar}}/\text{COOH} + \text{C}_{\text{ar}}$ ratio increased with an increasing pyrolysis temperature (Table 5) and was a suitable index for assessing the degree of maturation of coal organic matter.^{12,47}

3.4.4. Changes in Aromatic Hydrogen Structures. Three out-of-plane $\text{C}-\text{H}$ deformation bands were observed in the $900\text{--}700\text{ cm}^{-1}$ region for both coals. The bands near 870 , 815 , and 750 cm^{-1} in the original spectra were assigned to aromatic structures with isolated aromatic hydrogen atoms, two adjacent hydrogen atoms per ring, and four adjacent aromatic hydrogen atoms, respectively.^{12,13,57,58} The band positions and assignments in the FTIR spectra of lignite samples are given in Table 3. The degree of aromatic substitution and condensation with increasing pyrolysis temperature could be estimated by the number of adjacent hydrogen atoms per ring.⁶ The variations of the three main bands have been used to study the changes in the aromatic hydrogen structures during pyrolysis, and the results are reported in Table 6. For chars prepared at temperatures between 350 and 650 °C , the extent of aromatic substitution for HL coal seemed to decrease with increasing temperature, as demonstrated by the increase in the $770\text{--}700\text{ cm}^{-1}$ zone and the decrease in the $830\text{--}770$ and $900\text{--}830\text{ cm}^{-1}$ zones. For YN chars, the intensity of the $830\text{--}770\text{ cm}^{-1}$ and $770\text{--}700\text{ cm}^{-1}$ zones decreased with increasing temperature and the intensity of the $900\text{--}830\text{ cm}^{-1}$ zone began to increase at around 350 °C and declined at around 500 °C . This indicated that larger aromatic rings formed with aromatic substitution decreasing during pyrolysis. These larger aromatic ring groups can cross-link with the rest of the char structures.⁵⁶ Below 350 °C , these three deformation bands decreased for studied coals and the aromaticity decreased markedly (Table 6), possibly because of the formation of highly substituted aromatic rings or larger ring sizes. For the char prepared at 450 °C from HL coal, the intensity of all three deformation bands increased (Table 6) because of breakage of the coal macromolecular network, resulting in volatile matter release (Figure 4) and subsequent stabilization of free radicals by the hydrogen produced in pyrolysis. At temperatures above 650 °C , the $900\text{--}830\text{ cm}^{-1}$ zone increased with increasing temperature for both coals, indicating the increased degree of aromatic condensation and formation of a large amount of condensed aromatic nuclei. Carbonization at higher temperatures enhanced the stability of polycyclic aromatic components of the carbon structure as a result of decomposition of aromatic CH components and $\text{C}-\text{O}$ species.⁵⁵

4. CONCLUSION

During low-temperature pyrolysis of lignite, the char yield decreased rapidly, while the gas yields increased monotonically with increasing temperature in pyrolysis below 450 °C . The tar

Table 6. Evolution of the Aromatic C–H Out-of-Plane Deformation Zone^a

type ^b	sample	raw coal	char preparation temperature (°C)								
			350	400	450	500	550	600	650	700	750
1H ^c	HL	1.45	0.91	0.47	0.65	0.08	0.10	0.11	0.18	0.29	0.62
	YN	0.93	0.21	0.22	0.33	0.16	0.18	0.16	0.28	0.65	0.75
2H, 3H ^d	HL	0.66	0.42	0.39	0.49	0.19	0.12	0.05	0.21	0.22	0.23
	YN	1.26	0.67	0.80	0.42	0.36	0.16	0.16	0.23	0.23	0.41
4H, 5H ^e	HL	0.83	0.14	0.17	0.23	0.16	0.21	0.25	0.35	0.11	0.13
	YN	0.39	0.23	0.21	0.11	0.20	0.07	0.10	0.15	0.13	0.07

^aIntegrated absorbance area = absorbance units × cm⁻¹. ^bNumber of adjacent aromatic hydrogens per ring. ^cThe 900–830 cm⁻¹ zone. ^dThe 830–770 cm⁻¹ zone. ^eThe 770–700 cm⁻¹ zone.

yield increased to its maximum at 550 °C and decreased thereafter. The volatile matter release became more intensive with increasing temperature, resulting in cracks and open pores on the surface of char particles. With increasing the pyrolysis temperature, the decreased volatile matter content in char led to an increase in the ignition temperature. The combustion reactivity of low-temperature chars was greater than that of corresponding raw coals and the high-temperature chars, which can be attributed to the greater concentration of active surface sites and the lower degree of structural order.

Aliphatic structures and oxygen-containing functional groups of char decreased preferentially as the pyrolysis temperature increased. The tightly bound cyclic OH tetramers and OH–ether O hydrogen bonds were stronger than other hydrogen bonds in the 3700–3600 cm⁻¹ region. HL coal had a larger number of alkyl chains than that of YN coal according to the CH₃/CH₂ ratio, and a higher tar production was observed for HL coal. The cross-linking for YN coal seemed to occur at lower temperatures compared to HL coal, resulting in a lower tar yield. The C_{ar}/C=O + C_{ar} ratio increased with increasing the temperature of pyrolysis.

AUTHOR INFORMATION

Corresponding Author

*Telephone: +86-412-5929105. Fax: +86-412-5929627. E-mail: jianglongyu@163.com.

Notes

The authors declare no competing financial interest.

ACKNOWLEDGMENTS

This study was supported by the Natural Science Foundation of China (21176109, U1361120 and 21210102058). The authors also acknowledge the financial support of the Australia–China Joint Coordination Group (JCG) on Clean Coal Technology Research and Development Grants and the Liaoning Outstanding Professorship Program (2011).

REFERENCES

- (1) Skodras, G.; Natas, P.; Basinas, P.; Sakellaropoulos, G. P. Effects of pyrolysis temperature, residence time on the reactivity of clean coals produced from poor quality coals. *Global NEST J.* **2006**, *8*, 89–94.
- (2) Roberts, R. M.; Sweeney, K. M. Low-temperature pyrolysis of Texas lignite, basic extracts and some related model compounds. *Fuel* **1984**, *63*, 904–908.
- (3) Haykiri-Acma, H.; Yaman, S.; Kucukbayrak, S. Effect of pyrolysis temperature on burning reactivity of lignite char. *Energy Educ. Sci. Technol., Part A* **2012**, *29*, 1203–1216.
- (4) Khan, M. R. Significance of char active surface area for appraising the reactivity of low- and high-temperature chars. *Fuel* **1987**, *66*, 1626–1634.
- (5) Xie, K. C. *Coal Structure and Its Reactivity*; Science Press: Beijing, China, 2002.
- (6) Ibarra, J.; Moliner, R.; Bonet, A. J. FT-i.r. investigation on char formation during the early stages of coal pyrolysis. *Fuel* **1994**, *73*, 918–924.
- (7) Alonso, M. J. G.; Borrego, A. G.; Alvarez, D.; Menéndez, R. Pyrolysis behaviour of pulverised coals at different temperatures. *Fuel* **1999**, *78*, 1501–1513.
- (8) Sheng, C. Char structure characterised by Raman spectroscopy and its correlations with combustion reactivity. *Fuel* **2007**, *86*, 2316–2324.
- (9) Bend, S. L.; Edwards, I. A. S.; Marsh, H. The influence of rank upon char morphology and combustion. *Fuel* **1992**, *71*, 493–501.
- (10) Cai, H. Y.; Güell, A. J.; Chatzakis, I. N.; Lim, J. Y.; Dugwell, D. R.; Kandiyoti, R. Combustion reactivity and morphological change in coal chars: Effect of pyrolysis temperature, heating rate and pressure. *Fuel* **1996**, *75*, 15–24.
- (11) Yu, J.; Lucas, J. A.; Wall, T. F. Formation of the structure of chars during devolatilization of pulverized coal and its thermoproperties: A review. *Prog. Energy Combust. Sci.* **2007**, *33*, 135–170.
- (12) Ibarra, J.; Muñoz, E.; Moliner, R. FTIR study of the evolution of coal structure during the coalification process. *Org. Geochem.* **1996**, *24*, 725–735.
- (13) Wang, S.-H.; Griffiths, P. R. Resolution enhancement of diffuse reflectance i.r. spectra of coals by Fourier self-deconvolution: 1. C–H stretching and bending modes. *Fuel* **1985**, *64*, 229–236.
- (14) Michaelian, K. H.; Friesen, W. I. Photoacoustic FT-i.r. spectra of separated western Canadian coal macerals: Analysis of the CH stretching region by curve-fitting and deconvolution. *Fuel* **1990**, *69*, 1271–1275.
- (15) Solomon, P. R.; Serio, M. A.; Despande, G. V.; Kroo, E. Cross-linking reactions during coal conversion. *Energy Fuels* **1990**, *4*, 42–54.
- (16) Taulbee, D. N.; Sparks, J.; Robl, T. L. Application of hot stage micro-FT-i.r. to the study of organic functional group changes during pyrolysis. *Fuel* **1994**, *73*, 1551–1556.
- (17) Tahmasebi, A.; Yu, J.; Han, Y.; Yin, F.; Bhattacharya, S.; Stokie, D. Study of chemical structure changes of Chinese lignite upon drying in superheated steam, microwave, and hot air. *Energy Fuels* **2012**, *26*, 3651–3660.
- (18) Mastral, A. M.; Rubio, B.; Membrado, L.; Fañanás, F. J. Coal conversion into char: A study of the initial steps. *Carbon* **1990**, *28*, 65–69.
- (19) Ibarra, J.; Moliner, R.; Gavilán, M. P. Functional group dependence of cross-linking reactions during pyrolysis of coal. *Fuel* **1991**, *70*, 408–413.
- (20) Jing-biao, Y.; Ning-sheng, C. A. I. A TG-FTIR study on catalytic pyrolysis of coal. *J. Fuel Chem. Technol.* **2006**, *34*, 650–654.
- (21) Wells, W. F.; Smoot, L. D. Relation between reactivity and structure for coals and chars. *Fuel* **1991**, *70*, 454–458.
- (22) Sadhukhan, A. K.; Gupta, P.; Saha, R. K. Characterization of porous structure of coal char from a single devolatilized coal particle: Coal combustion in a fluidized bed. *Fuel Process. Technol.* **2009**, *90*, 692–700.

- (23) Zhao, Y. Pyrolysis behavior of weakly reductive coals from northwest China. Ph.D. Thesis, Dalian University of Technology, Dalian, China, 2010.
- (24) Zhao, Y.; Hu, H.; Jin, L.; He, X.; Wu, B. Pyrolysis behavior of vitrinite and inertinite from Chinese Pingshuo coal by TG-MS and in a fixed bed reactor. *Fuel Process. Technol.* **2011**, *92*, 780–786.
- (25) Takarada, T.; Tamai, Y.; Tomita, A. Reactivities of 34 coals under steam gasification. *Fuel* **1985**, *64*, 1438–1442.
- (26) Sawettaporn, S.; Bunyakiat, K.; Kitayanan, B. CO₂ gasification of Thai coal chars: Kinetics and reactivity studies. *Korean J. Chem. Eng.* **2009**, *26*, 1009–1015.
- (27) Tahmasebi, A.; Yu, J.; Han, Y.; Li, X. A study of chemical structure changes of Chinese lignite during fluidized-bed drying in nitrogen and air. *Fuel Process. Technol.* **2012**, *101*, 85–93.
- (28) Painter, P. C.; Sobkowiak, M.; Youtcheff, J. FT-i.r. study of hydrogen bonding in coal. *Fuel* **1987**, *66*, 973–978.
- (29) Miura, K.; Mae, K.; Li, W.; Kusakawa, T.; Morozumi, F.; Kumano, A. Estimation of hydrogen bond distribution in coal through the analysis of OH stretching bands in diffuse reflectance infrared spectrum measured by in-situ technique. *Energy Fuels* **2001**, *15*, 599–610.
- (30) Miura, K.; Mae, K.; Morozumi, F.-a. A new method estimate hydrogen bondings in coal by utilizing FTIR and DSC. *Prepr. Pap.—Am. Chem. Soc., Div. Fuel Chem.* **1997**, *42*, 209–213.
- (31) Painter, P. C.; Coleman, M. M.; Jenkins, R. G.; Whang, P. W.; Walker, P. L., Jr. Fourier transform infrared study of mineral matter in coal. A novel method for quantitative mineralogical analysis. *Fuel* **1978**, *57*, 337–344.
- (32) Painter, P. C.; Snyder, R. W.; Youtcheff, J.; Given, P. H.; Gong, H.; Suhr, N. Analysis of kaolinite in coal by infrared spectroscopy. *Fuel* **1980**, *59*, 364–366.
- (33) Finkelman, R. B.; Fiene, F. L.; Painter, P. C. Determination of kaolinite in coal by infrared spectroscopy—A comment. *Fuel* **1981**, *60*, 643–644.
- (34) Solomon, P. R.; Carangelo, R. M. FTIR analysis of coal. 1. Techniques and determination of hydroxyl concentrations. *Fuel* **1982**, *61*, 663–669.
- (35) Solomon, P. R.; Carangelo, R. M. FT-i.r. analysis of coal: 2. Aliphatic and aromatic hydrogen concentration. *Fuel* **1988**, *67*, 949–959.
- (36) Shchipko, M. L.; Kuznetsov, B. N. Influence of the origin of chars, produced from lignite by different methods, on features of their activation process. *Fuel* **1998**, *77*, 527–532.
- (37) Li, C.-Z.; Bartle, K. D.; Kandiyoti, R. Characterization of tars from variable heating rate pyrolysis of maceral concentrates. *Fuel* **1993**, *72*, 3–11.
- (38) Megaritis, A.; Messenböck, R. C.; Chatzakis, I. N.; Dugwell, D. R.; Kandiyoti, R. High-pressure pyrolysis and CO₂-gasification of coal maceral concentrates: Conversions and char combustion reactivities. *Fuel* **1999**, *78*, 871–882.
- (39) Li, C.-Z.; Bartle, K. D.; Kandiyoti, R. Vacuum pyrolysis of maceral concentrates in a wire-mesh reactor. *Fuel* **1993**, *72*, 1459–1468.
- (40) Sharma, R. K.; Wooten, J. B.; Baliga, V. L.; Lin, X.; Chan, W. G.; Hajaligol, M. R. Characterization of chars from pyrolysis of lignin. *Fuel* **2004**, *83*, 1469–1482.
- (41) Lu, L.; Kong, C.; Sahajwalla, V.; Harris, D. Char structural ordering during pyrolysis and combustion and its influence on char reactivity. *Fuel* **2002**, *81*, 1215–1225.
- (42) Wang, J.; Du, J.; Chang, L.; Xie, K. Study on the structure and pyrolysis characteristics of Chinese western coals. *Fuel Process. Technol.* **2010**, *91*, 430–433.
- (43) Ludvig, M. M.; Gard, G. L.; Emmett, P. H. Use of controlled oxidation to increase the surface area of coal: Application to a bituminous and a semi-anthracite coal. *Fuel* **1983**, *62*, 1393–1396.
- (44) Alonso, M. J. G.; Borrego, A. G.; Alvarez, D.; Parra, J. B.; Menéndez, R. Influence of pyrolysis temperature on char optical texture and reactivity. *J. Anal. Appl. Pyrolysis* **2001**, *58*–*59*, 887–909.
- (45) Cai, H. Y.; Güell, A. J.; Chatzakis, I. N.; Lim, J. Y.; Dugwell, D. R.; Kandiyoti, R. Combustion reactivity and morphological change in coal chars: Effect of pyrolysis temperature, heating rate and pressure. *Fuel* **1996**, *75*, 15–24.
- (46) Nsakala, N. Y.; Essenhoff, R. H.; Walker, P. L., Jr. Characteristics of chars produced from lignites by pyrolysis at 808 °C following rapid heating. *Fuel* **1978**, *57*, 605–611.
- (47) Kister, J.; Giuliano, M.; Largeau, C.; Derenne, S.; Casadevall, E. Characterization of chemical structure, degree of maturation and oil potential of Torbanites (type I kerogens) by quantitative FT-i.r. spectroscopy. *Fuel* **1990**, *69*, 1356–1361.
- (48) Georgakopoulos, A. Study of low rank Greek coals using FTIR spectroscopy. *Energy Sources* **2003**, *25*, 995–1005.
- (49) Geng, W.; Nakajima, T.; Takanashi, H.; Ohki, A. Analysis of carboxyl group in coal and coal aromaticity by Fourier transform infrared (FT-IR) spectrometry. *Fuel* **2009**, *88*, 139–144.
- (50) Pandolfo, A. G.; Johns, R. B.; Dyrkacz, G. R.; Buchanan, A. S. Separation and preliminary characterization of high-purity maceral group fractions from an Australian bituminous coal. *Energy Fuels* **1988**, *2*, 657–662.
- (51) Solomon, P. R.; Hamblen, D. G.; Carangelo, R. M.; Serio, M. A.; Deshpande, G. V. General model of coal devolatilization. *Energy Fuels* **1988**, *2*, 405–422.
- (52) Solomon, P. R.; Hamblen, D. G.; Carangelo, R. M.; Serio, M. A.; Deshpande, G. V. Models of tar formation during coal devolatilization. *Combust. Flame* **1988**, *71*, 137–146.
- (53) Zawadzki, J. IR spectroscopy studies of oxygen surface compounds on carbon. *Carbon* **1978**, *16*, 491–497.
- (54) Lievens, C.; Mourant, D.; He, M.; Gunawan, R.; Li, X.; Li, C.-Z. An FT-IR spectroscopic study of carbonyl functionalities in bio-oils. *Fuel* **2011**, *90*, 3417–3423.
- (55) Meldrum, B. J.; Rochester, C. H. Infrared spectra of carbonaceous chars under carbonization and oxidation conditions. *Fuel* **1991**, *70*, 57–63.
- (56) Li, X.; Hayashi, J.-i.; Li, C.-Z. FT-Raman spectroscopic study of the evolution of char structure during the pyrolysis of a Victorian brown coal. *Fuel* **2006**, *85*, 1700–1707.
- (57) Yen, T. F.; Wu, W. H.; Chilingar, G. V. A study of the structure of petroleum asphaltenes and related substances by infrared spectroscopy. *Energy Sources* **1984**, *7*, 203–235.
- (58) Painter, P. C.; Coleman, M. M. Application of Fourier-transform infrared spectroscopy to the characterization of fractionated coal liquids. *Fuel* **1979**, *58*, 301–308.